American Journal of Applied Sciences 5 (8): 997-1004, 2008
ISSN 1546-9239

Estimation of C*-Integral for Radial Cracks in Annular Discs under Constant Angular Velocity and Internal Pressure

A.R. Gowhari-Anaraki, F. Djavanroodi and S. Shadlou
Department of Mechanical Engineering, Iran University of Science and Technology, Tehran, Iran

Abstract: The finite element method has been used to predict the creep rupture parameter, C*-Integral for single and double-edge cracks in eight annular rotating discs under constant angular velocity with and without internal pressure. In this study, a new dimensionless creeping crack configuration factor, Q* has been introduced. Power law creeping finite element analyses have been performed and the results are presented in the form of Q* for a wide range of components and crack geometry parameters. These parameters are chosen to be representative of typical practical situations and have been determined from evidence presented in the open literature. The extensive range of Q* obtained from the analyses are then used to obtain equivalent prediction equations using a statistical multiple non-linear regression model. The predictive equations for Q*, can also be used easily to calculate the C*-Integral values for extensive range of geometric parameters. The C*-Integral values obtained from predictive equations were also compared with those obtained from reference stress method (RSM). Finally, creep zone growth behavior was studied in the component during transient time.

Key words: Radial cracks, annular discs, constant angular velocity, internal pressure, creep zone

INTRODUCTION

In spite of wide ranging applications of rotating discs, relatively very little information on the resulting stress intensity factor is available and for C*-Integral there is not any comprehensive information for rotational discs. This parameter is significant in the determination of crack driving force, rate of crack growth and crack tip stress fields.

Stress Intensity Factor in rotating disc for different kind of cracks has been reported in references[1-13]. Moreover, fatigue crack growth in rotational disc had studied and the results were reported in references[14,15]. The size and the number of pie-sector shaped fragments produced at the failure of a rotating flat disk contain a radial through-thickness crack have been determined in the reference[16].

In this study by the analogy with the J-Integral a new relation for the C*-Integral has been suggested. For this purpose, a new dimensionless creeping crack configuration factor, Q*, has been defined in analogy with fracture crack configuration factor, Q as follows:

$$J = f\left(Q, \sigma_0, a, E\right) \quad (1)$$

$$C^* = f\left(Q^*, \sigma_0, a, n\right) \quad (2)$$

Where σ_0 and a are nominal stress and crack length, respectively. E and n are material modulus of elasticity and material creep properties, respectively.

In the present study, an extensive range of configure single- and double-edge cracks in annular rotating discs under constant angular velocity with and without internal pressure, is used to obtained equivalent prediction equations using a statistical multiple non-linear regression model[17]. The accuracy of this model is measured using a multiple coefficient of determination R^2 where $0 \le R^2 \le 1$. This coefficient is found to be greater than or equal to 0.98 for all cases considered in this study, demonstrating the quality of the model fit to the data. These equations can be used to obtain C* values that are based on the geometries and material properties being considered. In addition, comparison has been made between the results obtained from FEM with the results from RSM (reference stress method) for some cases. It is also suggested that one of the component configurations (i.e. the cracked slit rotating disc) can be selected as a suitable experimental sample to measure the real C*-Integral of rotating

Corresponding Author: F. Djavanroodi, Department of Mechanical Engineering, Iran University of Science and Technology, Tehran, Iran

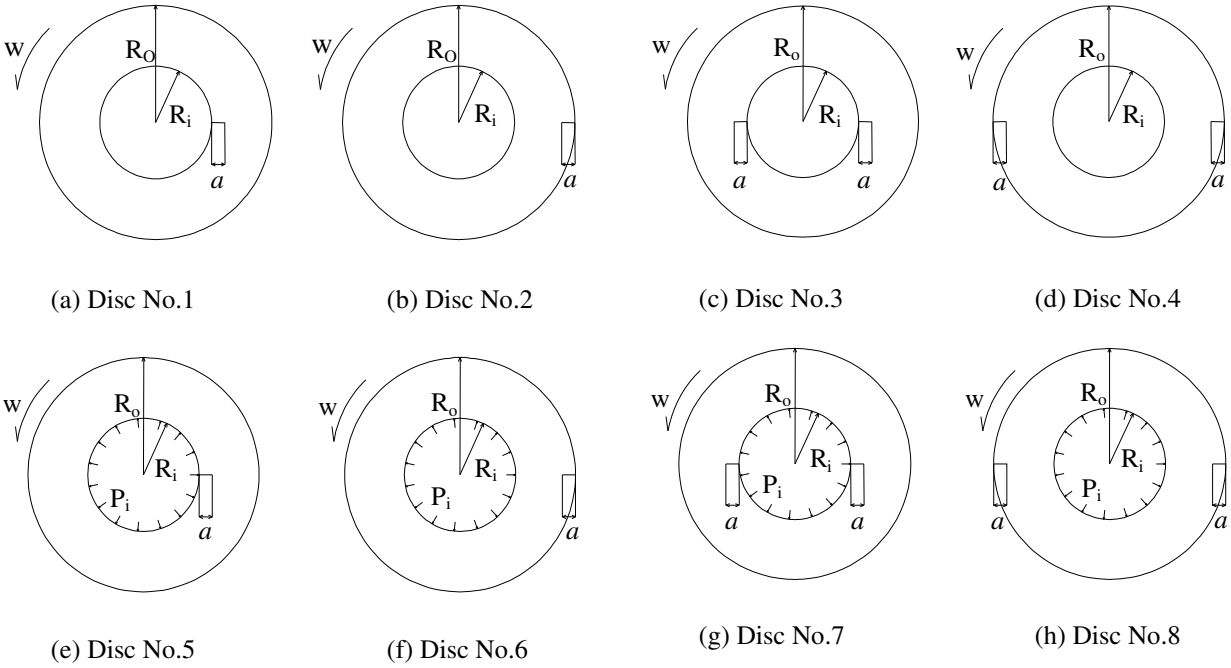

(a) Disc No.1 (b) Disc No.2 (c) Disc No.3 (d) Disc No.4

(e) Disc No.5 (f) Disc No.6 (g) Disc No.7 (h) Disc No.8

Fig. 1: Component geometry and loading condition

components, using the relevant predictive equation presented in this study.

Predictive equations for C*-Integrals enable designers to predict rate of crack growth easily. In addition, the effect of variation in geometrical parameter of the annular rotating disc components on Q* and, creep zone growth in the component during transient time were considered.

GEOMETRY AND LOADING CONDITIONS

Three dimensions are used to define the geometry as shown in Fig. 1. They are the internal radius R_i, the external radius R_O and the crack length a. Two non-dimensional parameters are formed by normalizing with respect to the external radius R_O, namely

$$\frac{R_i}{R_O}, \frac{a}{R_O}$$

The range of dimensions selected for the parametric study is consistent with the geometric cases covered by the Engineering Science Data Unit and used in references[18,19]. This is considered to present a range of practical interest. The selected ranges are

$$0 < \frac{a}{R_o} \leq 0.9$$

$$0.35 \leq \frac{R_i}{R_o} \leq 0.95$$

Eight components, rotating under constant angular velocity ω are considered in this study:

Disc 1: annular rotating disc, containing an internal radial single-edge through-crack (Fig. 1a)

Disc 2: annular rotating disc, containing an external radial single-edge through-crack (Fig. 1b)

Disc 3: annular rotating disc, containing an internal radial double-edge through-crack (Fig. 1c)

Disc 4: annular rotating disc, containing an external radial double-edge through-crack (Fig. 1d)

Disc 5: annular rotating disc, containing an internal radial single-edge through-crack with internal pressure (Fig. 1e)

Disc 6: annular rotating disc, containing an external radial single-edge through-crack with internal pressure (Fig. 1f)

Disc 7: annular rotating disc, containing an internal radial double-edge through-crack with internal pressure (Fig. 1g)

Disc 8: annular rotating disc, containing an external radial double-edge through-crack with internal pressure (Fig. 1h)

FINITE ELEMENT ANALYSIS

Finite element predictions have been obtained using ABAQUS[20]. Six- and eight-noded reduced integration, plane stress, triangular and quadrilateral elements were used with the crack tip singularity represented by collapsing one side of a quadrilateral to form a triangular element so that we have three points in crack tip. A typical finite element mesh is shown in Fig. 2. Due to lack of creep crack study in rotational annular disc, at first, some elastic finite element Analyses were used and the results were compared with data available in reference[1]. This comparison confirmed that the level of mesh refinement and the use of the crack tip elements in current study would provide accuracy to within ±4 percent.

Values for Young's modulus, material density and Poisson's ratio are, 209 GPa, 7840kg m^{-3} and 0.3, respectively and has been used throughout the analysis.

In creep situation, Strain was assumed to obey Bailey-Norton creep law.

$$\dot{\varepsilon} = A\sigma^{n} \tag{3}$$

The material creep properties for Rene 80, used in Bailey-Norton creep model are shown in Table 1.

RESULTS AND DISCUSSION

The C*-Integral values based on FE analysis: The C*-Integral values have been obtained using a numerical procedure based on the Virtual Crack Extension Method (VCEM) suggested by Landes and Begley[21], as follows:

$$C^{*} = \int_{\Gamma}^{0} w^{*} dy - T_{i}\left(\frac{\partial \dot{u}_{i}}{\partial x}\right) ds \tag{4}$$

Where

$$W^{*} = \int_{0}^{\dot{\varepsilon}_{y}} \sigma_{ij}\, d\dot{\varepsilon}_{ij} \tag{5}$$

Γ is a line contour shown in Fig. 3 taken counterclockwise from the lower crack surface to the upper crack surface. W* is the strain energy rate density associated with the point stress, σ_{ij} and strain rate $\dot{\varepsilon}_{ij}$. T_i is the traction vector defined by the outward normal, n_j, along Γ. In this section, the VCEM procedure incorporated in the ABAQUS[20] finite element program has been used to calculate the C*-Integral values.

Table 1: Material creep properties and rupture stress for Rene 80

1150	930	650	T (°C)
16.272×10^{-3}	6.37×10^{-5}	1.855×10^{-6}	$A\left(\frac{1}{(Mpa)^{n}\, hr}\right)$
1.43	4.6	2.54	n
165	170	175	σ_{R} (MPa)

Table 2: Normalized C*-Integrals for typical contour paths

3	2	1	Contour
0.983	0.991	1	C^{*} Normalized

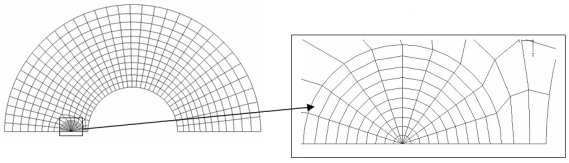

Fig. 2: Typical finite element mesh

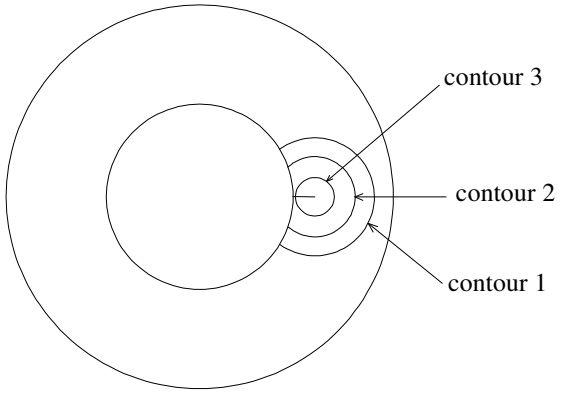

Fig. 3: C*-Integral contour paths

It has been shown in reference[22] that the value of C* is independent of the path Γ if the path originates at any point on the lower crack surface and goes counterclockwise and ends at any point on the upper crack surface.

In order to validate our predictions based on FEM, C*-Integral values have been obtained using three separate contours around the crack tip, which are shown in Fig. 3 for a typical geometry. All contour integrals generally showed good path independence, as illustrated in Table 2 where the C* values are normalized with respect to the value for the outermost contour 1. Consequently, the values for contour 1 were used throughout this study.

Analytical equation for C*-Integral: The J-Integral is usually written as:

$$J = \frac{K_I^2}{E} \quad (6)$$

Where

$$K_I = F_C \sigma_0 \sqrt{\pi a} \quad (7)$$

Where F_c is the crack configuration factor that is function of geometry. Substitution of Eq. (7) into Eq. (6) gives:

$$J = \frac{F_c^2 \pi}{E} \sigma_0^2 a \quad (8)$$

Or in a simple form:

$$J = Q \sigma_0^2 a \quad (9)$$

Where Q is called fracture configuration factor.

In this study a similar equation for C*-Integral has been introduced. To drive a new equation for C* it must consider that the relation between C* and nominal stress in creep situation is not linear. To determine the relation, many analyses have been done that kept constant all of the parameters and just changed the nominal stress. The relation between C* and nominal stress have found as follows

$$C^* \propto \sigma_0^{n+1} \quad (10)$$

Where n is material creep property. Therefore the relation between C* and nominal stress depends on creep behavior of material.

By the analogy with J-Integral and considering Eq. 10, the following equation for C* has been defined:

$$C^* = \frac{Q^* \sigma_0 a}{t_T} \left(\frac{\sigma_0}{0.01 \times \sigma_R} \right)^n \quad (11)$$

Where Q* is a non-dimensional parameter which is function of geometry and creep behavior of material and the equations related to each component are given in the following, σ_0 is nominal stress, σ_R is rapture stress of material, t_r is transition time and a is crack length.

To use this equation put transition time (t_r) equal 1000 h because this time has been considered in the analysis. Amounts of rupture stress (σ_R) are shown in Table 1 for different temperatures so the average amount has been used in this study so put rapture stress (σ_R) equal 170 MPa. This parameter has been used just to keep equation right, dimensionally. For all the components without internal pressure, the nominal stress σ_0 can be defined as:

$$\sigma_0 = \frac{3+\upsilon}{4} \rho \omega^2 R_o^2 \left[1 + \frac{1-\upsilon}{3+\upsilon} \left(\frac{R_i}{R_o} \right)^2 \right] \quad (12)$$

Where υ is Poisson's ratio and ω is angular velocity. Moreover, in cases that are subjected to internal pressure nominal stress can be defined as:

$$\sigma_0 = \sigma_\omega + \sigma_p \quad (13)$$

Where

$$\sigma_p = \frac{R_o^2 - R_i^2}{R_o^2 + R_i^2} \times P_i \quad (14)$$

$$\sigma_\omega = \frac{3+\upsilon}{4} \rho \omega^2 R_o^2 \left[1 + \frac{1-\upsilon}{3+\upsilon} \left(\frac{R_i}{R_o} \right)^2 \right] \quad (15)$$

Also creep crack growth rate da/dt and C* are related by the following relationship

$$\frac{da}{dt} = b \left(C^* \right)^q \quad (16)$$

Where b and q are material constants obtained from regression of the data and are related to the intercept and slope, respectively, of the da/dt vs. C* on a log-log plot. The values of b and q can change from material to material.

Comparison of C*-Integral values obtained from FEM and reference stress method (RSM).

It is recognized by present authors that the method of calculation C* based on reference stress is not necessarily very accurate, but in comparison with other methods is fast and relatively reliable.

When finite element solutions for C* are not available, the following equation can be employed for determining approximate estimates:

Table 3: Comparison of C* values obtained from FEM and Reference Stress Method ρ = 7840 Kg m^{-3}, w = 200 Rad s^{-1}

Deviation	P(MP*a*)	R_o(mm)	R_i(mm)	*a*(mm)	Temperature (°C)	C^*(Mpa.m h^{-1}) (RSM)	C^*(Mpa.m h^{-1}) (Eq. 11)	Disc No.
12%	---	10	3.5	1	1150	5.392×10^{-9}	4.743×10^{-9}	1
11%	---	10	6.5	1.2	650	2.25×10^{-12}	2.019×10^{-12}	2
16%	---	30	20	1.4	930	1.340×10^{-9}	3.809×10^{-9}	3
7%	---	35	15	0.5	930	2.451×10^{-9}	2.278×10^{-9}	4
14%	0.1	36	26	2	1150	2.65×10^{-6}	2.322×10^{-6}	5
10%	0.1	34	17	5	650	6.35×10^{-8}	5.748×10^{-8}	6
9%	0.1	40	22	6.5	650	10.714×10^{-7}	9.743×10^{-7}	7
11%	0.1	38	30	2.3	930	3.560×10^{-7}	3.229×10^{-7}	8

$$C^* = \sigma_{ref}\dot{\varepsilon}^c_{ref}\left(K/\sigma_{ref}\right)^2 \quad (17)$$

Where $\dot{\varepsilon}^c_{ref}$ is the total rate of strain obtained from the material stress-strain properties at the reference stress and K is stress intensity factor and σ_{ref} is reference stress. Before Eq. 17 can be evaluated, σ_{ref} must be obtained. It can be determined from limit analysis or numerical methods[23,24]. When limit analysis is employed, for a component subjected to a load P, reference stress is given by:

$$\sigma_{ref} = \sigma_y \frac{\sigma_0}{P_{LC}} \quad (18)$$

Where σ_y is the material yield stress and P_{LC} is the corresponding collapse load of the cracked component that in this study have obtained by FEM. Strain rate and stress relation can determine the reference strain rate as follow

$$\dot{\varepsilon}^c_{ref} = A\sigma^n_{ref} \quad (19)$$

The results were compared for eight different components that are shown in Table 3. It is seen that the agreement between two approaches is reasonably good and this suggests that the FEM results are correct.

As it is seen, the RSM is a simplified method so the results obtained from this method are over estimate.

TRANSITION TIME

Riedel and Rice in their original analyses presented a concept of transition time, T_t. They defined the transition time as the time when the small-scale-creep stress fields equal the extensive steady-state creep fields characterized by C*. Finite element analyses has been performed for time of more than 1000 hours to be insure that transition time has passed. Nonetheless, to examine the accuracy of this time the results for different timing duration were examined and as it was expected, no changes were occurred after a certain time,

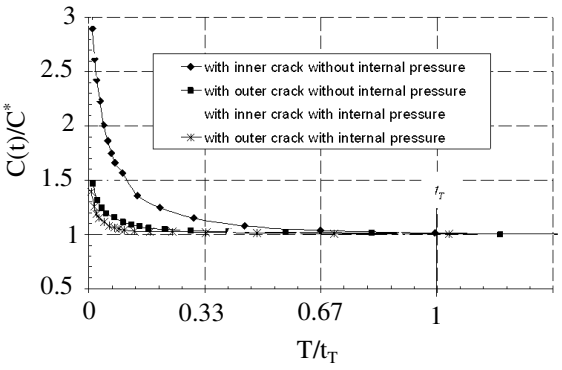

Fig. 4: The variation of normalized C(t) integral with respect to normalized time for T = 650°C, R_i/R_o = 0.65, *a* = 0.065

before 1000 hours. Figure 4 compare the transition time for different component, loading and times. In order to show all the results in one graph the vertical axis is normalized by C* and the horizontal axis are normalized by transition time.

Components that contains external crack, pass transition time faster than components with internal crack and the components with same crack position that are subjected to an internal pressure have shorter transition time than components without internal pressure.

CREEP ZONE SIZE

Riedel and Rice[25] arbitrarily defined the creep zone boundary as the locus of points where time-dependent effective creep strains equal the instantaneous effective elastic strains in the cracked body. Generally, the creep zone starts at some points with high stress concentration factor and growths to cover all the body. The creep zone in three steps is shown in Fig. 5. As it can be seen, the creep zone started from the crack tip that has maximum stress concentration in the body. Then the creep zone covers all inner edge of annular rotating disc.

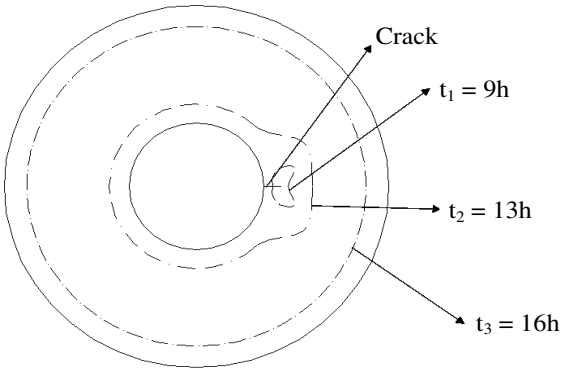

Fig. 5: A typical creep zone growth in annular rotating disc for rotating disc

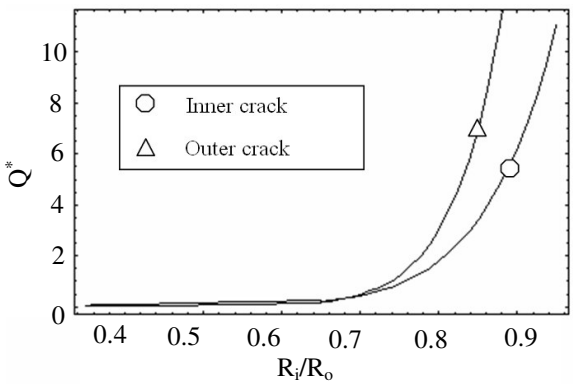

Fig. 6: Variation in Q* with R_i/R_o for T = 1150°C, $\frac{a}{R_o}=0.15, w=300\frac{Rad}{sec}, p=0$

This is because the inner edge of annular rotating disc has maximum amount of stress in all of the body if the crack is ignored.

VARIATION IN Q* WITH $R_i/R_o, a/R_o$

In order to understand how Q* varies with $R_i/R_o, a/R_o$, a number of calculations has been performed. This is important because it helps designer to choose the best geometry. Figs (6, 7) shows the variation of Q* with R_i/R_o for two kind of loading. As it can be seen for $R_i/R_O \geq 0.7$ the amount of Q* increase very fast. also before this point the amount of Q* for component with inner crack is higher than outer crack. Nevertheless, after this point the amount of Q* for component with outer crack is higher than those with inner crack.

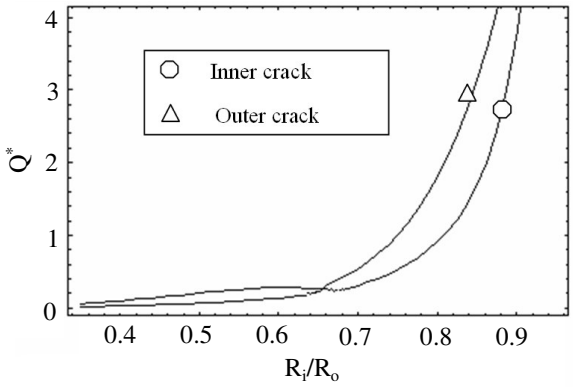

Fig. 7: Variation in Q* with R_i/R_o for $T=1150^oC, \frac{a}{R_o}=0.15, w=300\frac{Rad}{sec}, p=0.1MPa$

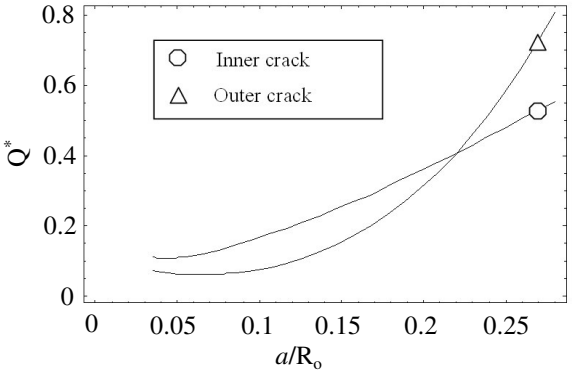

Fig. 8: Variation in Q* with a/R_o for $T=1150^oC, \frac{R_i}{R_o}=0.65, w=300\frac{Rad}{sec}, p=0$

This is because when the ratio of R_i/R_o is small for components with inner crack, the distance between crack tip and inner edge (with higher stress concentration in the body) is smaller than components with outer crack and it causes higher Q* and when the ratio of R_i/R_o is more than 0.7 vice versa.

Variation in Q* with a/R_o for two kind of loading is shown in figures (8, 9). It is shown that in the absent of internal pressure (Fig. 8) $a/R_O=0.23$ is threshold point and when there is internal pressure (Fig. 9) $a/R_O=0.2$ is threshold point, before these threshold points the amount of Q* for component with inner crack is higher than outer crack. Nevertheless, after this point the amount of Q* for component with outer crack is higher than inner crack.

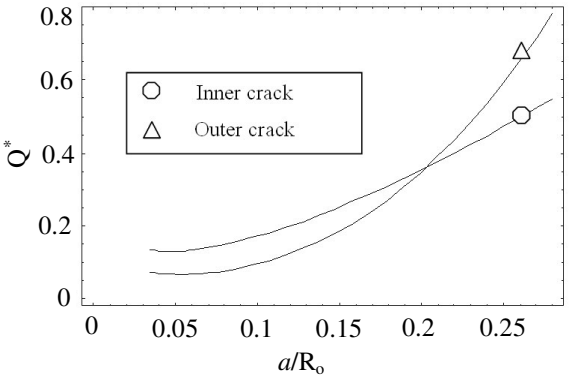

Fig. 9: Variation in Q* with a/R_o for $T = 1150^oC, \frac{R_i}{R_o} = 0.65, w = 250\frac{Rad}{sec}, p = 0.1MPa$

This is because for components with inner crack and small a/R_o, the distance between crack tip and inner edge (with higher stress concentration in the body) is smaller than components with outer crack and it causes higher Q* and when the ratio of a/R_o is more than 0.2 the opposite thing will happen.

CONCLUSION

It has been shown that the relation between C* and nominal stress σ_0 as $C^* \propto \sigma_0^{n+1}$. Also components with external crack or internal pressure has shorter transition time than components with internal crack or without internal pressure.

It has also been shown that Q* can be used to predict C*-Integral. Threshold points $R_i/R_O = 0.7$, $a/R_O = 0.23$ and $a/R_O = 0.2$ has been defined which are good tools for designing annular discs performing at high temperatures.

REFERENCES

1. Gowhari-Anaraki, A.R., S.J. Hardy and R. Adibi-Asl, 2004. Stress Intensity Factors for Radial Cracks in Annular and Solid Discs under Constant Angular Velocity. J. Strain Analysis., 38: 217-223.
2. Fett, T., 2002. Stress Intensity Factors and T-Stress for Single and Double-edge-Cracked Circular Disks under Mixed Boundary Conditions. Eng. Fract. Mech., 69: 69-83.
3. Fett, T., 2001. Stress Intensity Factors and T-Stress for Internally Cracked Circular Disks under Various Boundary Conditions. Eng. Fract. Mech., 68: 1119-1136.
4. Wilson, R.L. and S. A. Meguid, 1995. On the Determination of Mixed Mode Stress Intensity Factors of an Angled Crack in a Disc Using FEM. Finite Elem. Anal. Des., 18: 433-448.
5. Xu and L. Yong, 1993. Stress Intensity Factors of a Radial Crack in a Rotating Compound Disk. Eng. Fract. Mech., 44: 409-423.
6. Bell, R., I.A. Pagotto and J. Kirkhope, 1989. Evaluation of Stress Intensity Factors for Corner Cracked Turbine Discs under Arbitrary Loading Using Finite Element Methods. Eng. Fract. Mech., 32: 65-79.
7. Schneider, G.A. and R. Danzer, 1989. Calculation of the Stress Intensity Factor of an Edge Crack in a Finite Elastic Disc Using the Weight Function Method. Eng. Fract. Mech., 34: 547-552.
8. Rooke, D.P. and J. Tweed, 1988. Stress Intensity Factors for Periodic Radial Cracks in a Rotating Disc. Int. j. eng. Sci., 26: 1059-1069.
9. Jia, H. and C.L. Tan, 1985. Stress Intensity Factors for Corner Cracks in Rotating Discs. Int. J. Fracture., 28: R57-R62.
10. Smith, R.N.L., 1985. Stress Intensity Factors for an ARC Crack in a Rotating Disc. Eng. Fract. Mech., 21: 579-587.
11. Chen, W.H. and T.C. Lin, 1983. A Mixed-Mode Crack Analysis of Rotating Disk Using Finite Element Method. Eng. Fract. Mech., 18: 133-143.
12. Isida, M., 1981. Rotating Disk Containing an Internal Crack Located at an Arbitrary Position. Eng. Fract. Mech., 14: 549-555.
13. Rooke, D.P. and J. Tweed, 1973. The Stress Intensity Factor of an Edge Crack in a Finite Rotating Elastic Disc. Int. J. Eng. Sci., 11: 279-283.
14. Shlyannikov, V.N., B.V. Iltchenko and N.V. Stepanov, 2001. Fracture Analysis of Turbine Disks and Computational-Experimental Background of the Operational Decisions. Eng. Fail. Anal., (5): 461-475.
15. Zhuang, W.Z., 2000. Prediction of Crack Growth from Bolt Holes in a Disc. Int. J. Fatigue., 22: 241-250.
16. BERT, C.W. and T.K. PAUL, 1995. Failure Analysis of Rotating Discs. Inl. J. Soli and Stmcrures., 32: 1307-1318.
17. Mendenhall, W., J.E. Reinmuth and R. Beaver, 1989. Statistics for Management and Economics. 6th Ed., PWS-kent Publishing Company.

18. Rooke, D.P. and D.J. Cartwright, 1976. Compendium of Stress Intensity Factors. The Hillingdon Press, Uxbridge, Middlesex.
19. Tada, H., P.C. Paris and G.R. Irwin, 1986. The Stress Analysis of Cracks Handbook. Del Research Corporation, Hellertown, Pennsylvania.
20. ABAQUS Users manual, version 6.6-1, Inc. 2006.
21. Landes, J.D. and J.A. Begley, 1976. A Fracture Mechanics Approach to Creep Crack Growth. ASTM STP 590, pp: 128-148.
22. Saxena, A., 1998. Nonlinear Fracture Mechanics for Engineers. CRC Press, pp: 309-362.
23. Webster, G.A. and R.A. Ainsworth, 1994. High Temperature Component Life Assessment. London: Chapman and Hall.
24. Sim, R.G., 1971. Evaluation of Reference Parameters for Structures Subjected to Creep. J. Mech. Eng. Sci., 13: 47-50.
25. Riedel, H. and J.R. Rice, 1980. Tensile Cracks in Creeping Solids. Fracture Mechanics: Twelfth Conference, ASTM STP 700, American Society for Testing and Materials, pp: 112-130.